PAPER • **OPEN ACCESS**

Analysis of a Mechanical Anchoring System for Landing on Asteroids

Analysis of a Mechanical Anchoring System for Landing on Asteroids

Weimin Wang*, K. L. Yung

Department of Industrial and Systems Engineering, The Hong Kong Polytechnic University, Kowloon, Hong Kong SAR, People's Republic of China

Corresponding author's e-mail address: eewmwang@gmail.com

Abstract. The landing process to an asteroid is discussed with a Nimble Lander. The miniature harpoons are chosen as the anchoring device to landing to asteroid in the Nimble Lander. The analysis results provide detailed information of the anchoring with harpoon as anchoring device. Many different designs of harpoon have been tested by simulation, the best of three designs of harpoon are analyzed for anchoring to Apophis. Instead of the modelling of the anchor as a rigid cylindrical projectile in penetration models, the deformation of the harpoon is fully considered in the anchoring analysis. The analysis provides ground base a reliable design anchoring system for landing to Asteroids.

1. Introduction

Radar images of asteroid 308653 Apophis were obtained on Nov.8, 2011, with the closest approach of (0.845 lunar distances, 325000 km) flyby of Earth between 1976 and 2028.

Asteroid 99942 Apophis is estimated to have a 320 m diameter and a mass of 4.6×10^{10} Kg. Asteroid 99942 (Apophis) [1] has an unusually close approach to the Earth on Apr. 13, 2029. It will pass some 38,200 km from the Earth center and subsequently will be perturbed by the Earth's gravity into a new heliocentric orbit. Even if Apophis eventually does not impact the Earth, the high accuracy orbit determination efforts for this complicated case will certainly be made to similar cased in the future [1]. On Apr. 13, 2029, Apophis will pass the Earth so near that its trajectory around the Sun will be significantly altered by the gravitational pull from the Earth [2]. Depending on the actual perigee radius of this fly by, which is presently estimated with an uncertainty of several thousands of kilometres, Apophis will be moved on a new orbit, with a longer period, ranging between 417 and 427 days.

Several cost-based planning rendezvous with Apophis are proposed [3]-[5]. Little is known about properties of out-layer and internal composition of YU55 and Apophis, which is certainly important for counter-measure can be designed. The mission of sampling and necessary in situ exploration of the two asteroids are put forward.

Nathues et al. [6] presents a concept study of an in-situ exploration mission to two NEAs. Duffard et al. [7] propose a dual-rendezvous to NEAs, including sample-return. The landing strategies of Philae and other lander concepts are studied by Ulamec et al. [8]-[9]. Modeling as combination of spring and damping for each mechanism of the Rosetta Lander, the dynamics of the Rosetta Lander impact on comet surface in the frame of a multibody analysis is described by Hilchenbach et al. [10]. The early-stage design of anchoring harpoon for Rosetta Lander is presented by Thiel et al. [11]. The capabilities of Rosetta Lander, Philae, is reported by Biele et al. [12]. Kargl et al. [13] investigate the accelerometry

measurements using the Rosetta Lander's anchoring harpoon. The deceleration signal fitting according to penetration models is extensively reviewed by Komle et al. [14].

2. Mission and Spacecraft Design

In order not to interfere the orbit of Apophis, the Apophis lander design avoids using approaches involved with large impact energy. Therefore, anchoring harpoons are being used as the attaching method. By using this method, most impact (penetration) energy would be absorbed, minimizing the trajectory effect on the asteroid. Surface samples would be extracted and packaged. The sealed samples will be delivered to the spacecraft, which will return to Earth. The harpoon design of the Apophis lander is used in this study for penetration analysis.

3. Landing Process with the Nimble Lander

This paper focus on the stage of landing and sampling of Apophis in the mission. The mechanical, compositional and magnetic property of Apophis can be obtained with in situ analysis instruments. Such insight data can provide constitution and precise orbit of Apophis.

The anchoring harpoons are fired to Apophis when the Lander is approximately 2 meters to the surface of the asteroid. The landing process with anchoring harpoons is presented in Fig. 1. The Landing system shoots miniature 3 harpoons sequentially. The initial speed of harpoons shots to Apophis is 600 m/s, the orientation of Nimble Lander's base is modified by reaction force of every shot, while the three miniature harpoons are shot to Apophis surface in the normal direction. The speed and orientation of Lander base is adjusted properly after every shoot. The middle big harpoon is shot to the asteroid after the three miniature harpoons fail to anchor to Apophis. The big harpoon locating at centre of landing gear is shot with high velocity and self-rotating speed to anchor Apophis.

The Lander constitutes of a big harpoon and three miniature harpoons. The Lander has three advantages, (i) better penetration (smaller footprint); (ii) less impact force and better energy absorption (dispersed impact); (iii) better redundancy. The energy of the harpoon has to be absorbed through the penetration. The big harpoon locating at centre of landing gear acts as redundant anchoring device when the three miniature harpoons cannot anchor to Apophis properly. And the redundant compel engine start up to keep the Lander on the surface of the asteroid.

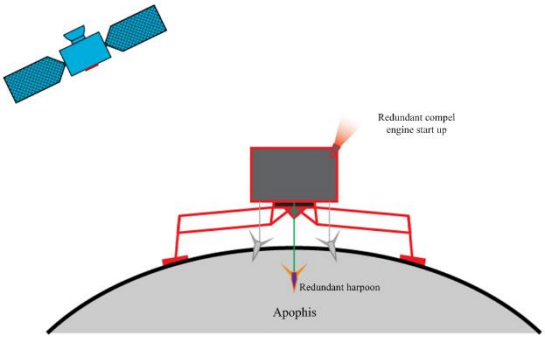

Figure 1. Touchdown of the Nimble Lander anchoring with miniature harpoons.

4. Simulations Anchoring of Philae by Harpoon

Rosetta is 16 km away from the comet 67P/Churyumov-Gerasimenko. The anchoring is investigated with finite element method to obtain detailed information about anchorage with harpoon devices. The advantage of choosing Philae to analyse is that it has rich design data and experiment data for the harpoon anchoring.

The numerical simulation results show both Foamglas T4 and Foamglas F material blocks can be anchored by the designed harpoon of Philae successfully. Fig. 2 shows the total deformation distribution of anchoring of Rosetta's harpoon into Foamglas F material 12 ms after shot. The comparison between computed results and experimental results is illustrated in Table 1. It can be seen the computed

penetration depth match well with the measured penetration depth. The error between computed and measured results mainly come from detailed design of anchoring harpoon of Rosetta cannot be obtained.

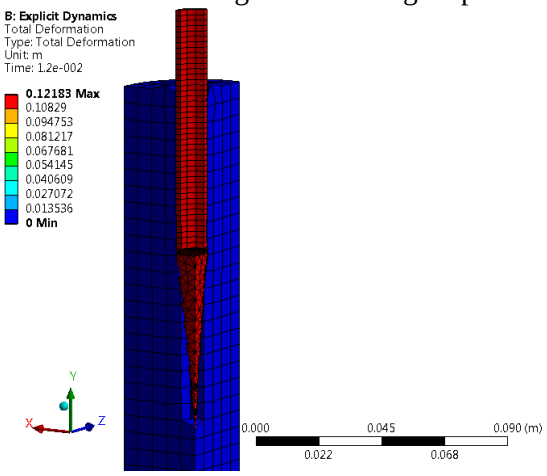

Figure 2. The anchorage of Rosetta harpoon into Foamglas F material.

Table 1. The Comparison between Computed Results and Measured Results for Rosetta Harpoon Shots

	Anchor mass (g)	Surface material	Initial velocity (m/s)	Free flight path (mm)	Penetration depth (mm)
Experiment (Komle et. al, [14])	71	Foamglas T4	38.7	250	210
	71	Foamglas F	38.9	230	120
Computed	67.2	Foamglas T4	38.8	1	228.6
	67.2	Foamglas F	38.8	1	117.4

5. Impact of Harpoon to Apophis

The anchoring harpoon is fired towards surface of Apophis to avoid rebound of the Lander at touch down Apophis.

5.1. Target Material for Apophis

The hypothesis of structure of asteroid is shown in Fig. 3 before the human landing to confirm the characteristics of the Apophis. The interior of the asteroid is composed of 4-6 large sized cores, and its outer surface is covered by a loose layer of regolith [15].

The estimated bulk density for regolith layer on other asteroids is our reference. Nolan et al. [16] derive the near surface bulk density of asteroid (101955) Bennu from radar combined with light curve data by two methods. The first, "uncalibrated" method extrapolated laboratory and planetary (Moon and Venus) scattering measurements to derive bulk density, the estimated bulk density is 1.65 g/cm3 for the asteroid Bennu. The second method simply assumes that Eros is a typical NEA and that bulk density scales linearly with the "opposite circular" to the transmitted circular polarization radar albedo, the estimated bulk density is 0.9 g/cm3 for Bennu. Chesley et al. [17], obtain an estimated of the bulk density of the entire asteroid to be approximately 1 g/cm3 from a measurement of the Yarkovsky effect on the

orbit of Bennu, though the uncertainties are large enough to prevent drawing any firm conclusions. The bulk density of regolith for Apophis is chosen as 1.65 g/cm3.

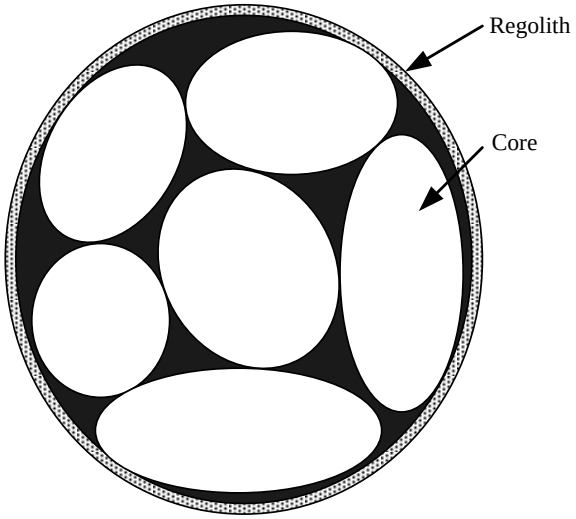

Figure 3. Model of Apophis for the Nimble Lander.

NASA's impact risk page listed the diameter of Apophis as 330 meters and the mass of the asteroid as 4×10^{10} kg based on an assumed density of 2.6 g/cm3. The estimation of mass is somewhat rougher than the estimation of diameter, but should be accurate to within a factor of three.

Apophis is found to be an Sq-class asteroid that most closely resembles LL ordinary chondrite meteorites in terms of spectral characteristics, a LL chondrite metrorite analog interpretation for Apophis is reported in [18]. Table 2 illustrates the known parameters for LL chondrite meteorites at the microscopic level.

Table 2. Range of Physical Parameters for (99942) (Adapted from Binzel et al, [18])

Parameter	Min	Avg	Max	Reference
Apophis diameter (m)	210	270	330	Delbo et al.[19]
Grain density (g/cm3)	3.4	3.5	3.6	Britt and Consolmagno [20]
Bulk density (g/cm3)	3.0	3.2	3.4	Britt and Consolmagno [20]
Micro-porosity (%)	3.7	7.9	12.1	Britt and Consolmagno [20]
Macro-porosity (%)	0	20	50	Britt et al. [21]
Calculations for Apophis				
Parameter	Min	Avg	Max	Itokawa-like
1-total porosity (micro+macro)	0.38	0.72	0.96	0.60
Mass ($\times10^{10}$ kg)	0.7	2.4	6.1	2.0

5.2. Numerical Simulations of Harpoon Fired to Apophis

Several different designs of the harpoon including the harpoon for Rosetta mission by simulation had tested. According to the above simulation studies, the best of the three designs have chosen as shown in Fig. 4 for an in-depth study.

The diameter of anchor shaft is 10 mm, the total height is 19.5 mm. Among the geometry models, the trapezoid-shaped blade is designed in Fig. 4 (a), the blade is designed to anchor to asteroid material. Fig. 4(b) shows the geometry model of two spring steel loops locate in the slot of tip, large elastic deformation property of the spring steel is used to avoid bounce off the harpoon. Fig. 4(c) shows the simple slot geometry model. The surface of asteroid is modelled with regolith layer and rock body. The upper layer is regolith, with diameter of 60 mm, height of 10 mm. The height of modelled rock is 100 mm.

In the numerical simulation, the impact is governed by the conservation of mass, momentum and energy, and also the strength model, equation-of-state and failure model of material. The strength model of material represents the material's resistance to shear. The equation-of-state of material considers the effects of compressibility of the material. The material properties of harpoon, regolith and rock are listed in the Table 3. The strength model of regolith is modelled as cohesionless granular material, which is modelled as zero Drucker-Prager strength stassi material in Ansys. The cores of Apophis are modeled as the LL chondrite material with porosity 7.9%. Drucker-Prager strength stassi model is defined for matrix chondrite strength model to consider change in shape. The density influence to yield stress and shear stress, pressure to yield stress can be considered in the strength model.

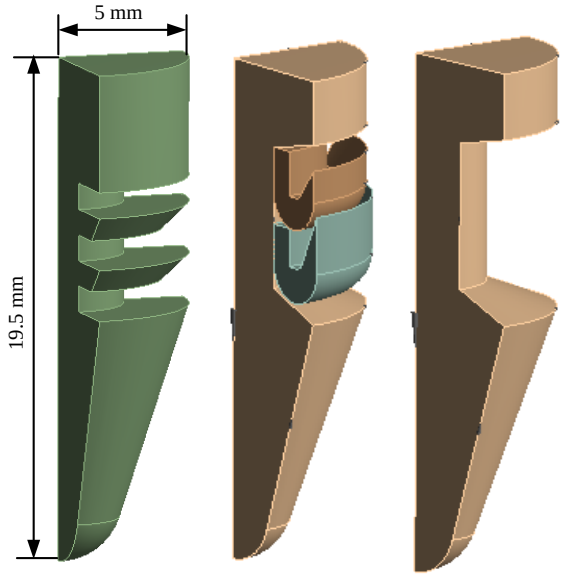

Figure 4. Geometry models of three different types of miniature harpoon designed for Apophis:(a) Trapezoid-shaped; (b) Spring steel; (c) Slot-shaped.

The numerical simulation is based on an explicit time-integration. The relation between mesh size and time-step is expressed with the Courant-Friedrich-Levy (CFL) criterion for an explicit time-integration.

$$\Delta t < \Delta x/c \quad (1)$$

where Δt is the time step, Δx is the smallest mesh size in the mesh, and c is sound velocity. Tetrahedral-shaped elements are meshed for harpoon model. The harpoon model is fine meshed for element. Hexahedral-shaped elements are meshed for the regolith and rock model. Note the tip of the

harpoon locates 1 mm above of regolith at the initial position. The initial speed of the miniature harpoon Vy is -600 m/s.

The fixed boundary condition is applied in the right edge of geometry model, and the acceleration that equal to 1/2000 conventional earth gravity is applied in the computation environment (Komle et al. [14]). The deceleration sensitivity variation to input parameters are studied in the penetration models. In the models, the anchor is considered to be a rigid, conically tipped cylindrical projectile. The coefficient of sliding friction between the rock and the surface of harpoon plays an important role to the deceleration profile. The fitting of the measured deceleration profiles shows the coefficient is small or zero to obtain good fits for the penetrated brittle material. It can be explained as the highly brittle body can not be compressed plastically before it fails due to collapse of the cell walls [14]. The crushed powder hides in the pores of the still intact environment and give no further contribution to the penetration resistance of the anchor [14]. In this study, the coefficient of sliding friction between the rock and the surface of the harpoon is chosen as 0.005.

To obtain the detailed directional deformation information of harpoon body (the spring steel is hidden), only harpoon body model is selected to show, the directional deformation along x axial for spring steel harpoon is depicted in Fig. 5. It can be seen some zone of harpoon body is broken with the high-speed impact; and the a few mesh of harpoon body are eroded in the computation, the red points are free mass points, i.e. free nodes of the eroded elements belong to harpoon body. The maximal x directional deformation exists at the blade zone and thin zone of the harpoon. The maximum directional deformation is 1.4 mm for harpoon with spring steel.

Fig. 6 shows the equivalent stress distribution while the harpoon penetrating into rock 12 ms after impact. The maximum equivalent stress locates at slot edge of harpoon with value 0.65 GPa.

The penetration depth for each node of a miniature harpoon is different for deformation variation existing for nodes of the harpoon. The selected node for reference of harpoon is shown in Fig. 7. The node locating at centre of top surface for each miniature harpoon is of our interest. The displacement and speed information of such node can be considered as penetration depth and velocity of harpoon. Fig. 8 shows the position variation of three types of miniature harpoon shooting to asteroid. It can be seen all miniature harpoons are bounced off within 1 ms after impact. The slot-shaped harpoon penetrates to the depth of 43 mm. The spring steel harpoon penetrates to the deepest position at 53 mm. The trapezoid-shaped harpoon penetrates to the depth of 59 mm.

Fig. 9 shows the velocity variation of three types of miniature harpoon. The trapezoid-shaped harpoon and slot-shaped harpoon decrease from 600 m/s to 0 m/s at 0.6 ms, while the spring-steel harpoon cease to move at 1 ms.

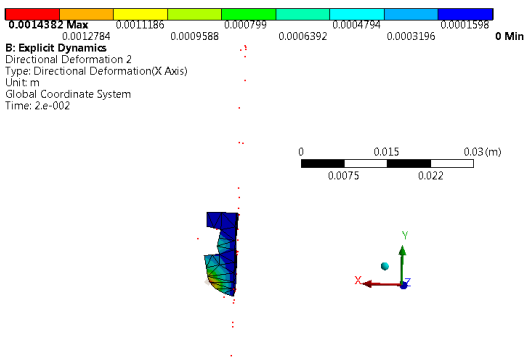

Figure 5. The x directional deformation distribution of the spring steel type harpoon 20 ms after impact.

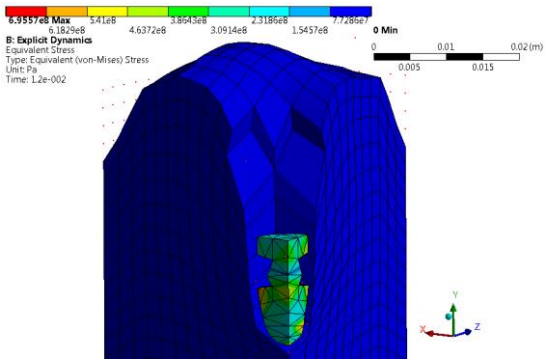

Figure 6. Equivalent stress distribution of a slot-shaped harpoon impact with rock 12 ms after impact.

Table 3. ANSYS Model Parameters for Harpoon Penetration

Regolith	
Density	1650 Kg/m3
Drucker-Prager Strength Stassi Model	
Shear Modulus	0.0279 GPa
Bulk Modulus	0.19 GPa
LL ordinary chondrite (from Kimberley et. al. [22]; Dai et. al. [23])	
Density	3350 Kg/m3
Drucker-Prager Strength Stassi Model	
Shear Modulus	1.333 GPa
Shock Equation of State Linear	
Porosity	7.9%
Strain, stress and crack softening Failure	
Harpoon Model : Material Steel 4340	
Density	7830 Kg/m3
Johnson Cook Strength	
Bulk Modulus	159 GPa
Shear Modulus	81.8 GPa
Johnson Cook Failure	

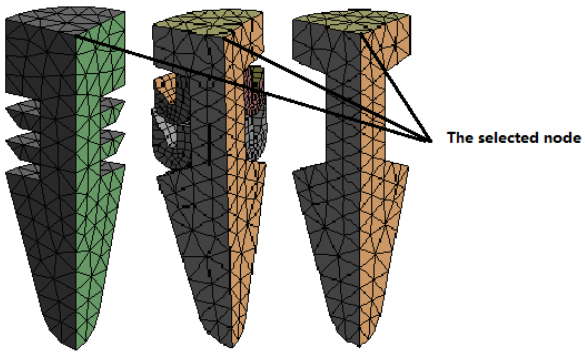

(a) (b) (c)

Figure 7. The selected node for the penetration information of the harpoon:(a) Trapezoid-shaped; (b) Spring steel; (c) Slot-shaped.

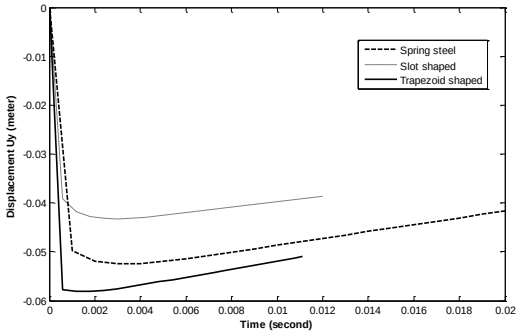

Figure 8. The position of the miniature harpoon with penetration.

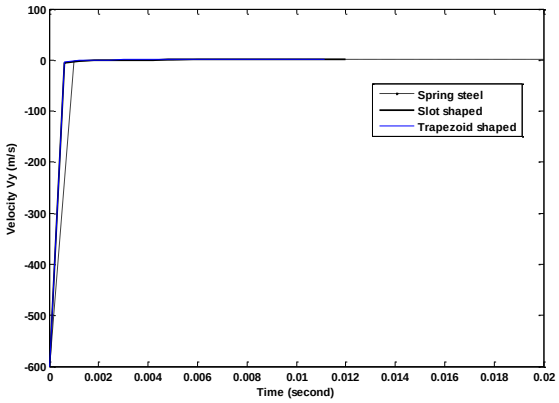

Figure 9. The velocity of the miniature harpoon with penetration.

5.3. Summary

The bounce off can be explained when the harpoons reach the deepest penetration position, for the designed harpoons, it is around 1 ms after impact.

A. The penetration depths of the harpoons to Apophis range from 43 to 59 mm.
B. There is void space around the body of harpoon, even the lower zone of blade is enlarged with deformation of harpoon. The diameter of penetrated hole is larger than the diameter of harpoon.
C. The shape of penetration hole of harpoon is alike the shape of meteorite crafter.
D. The bounce off is due to the reaction force of rock to tip of harpoons.

E. The failure anchoring of harpoon design is that the rock is brittle material. There is not obvious plastic property for the material. The rock behaves as a highly brittle body, which cannot be compressed plastically before it fails due to collapse of the material's cell wall.
F. Some rock material located down of harpoon is destroyed by the penetration of harpoon, the material erodes as isolated nodes, the nodes are displayed as red points in the harpoon computation.

6. Conclusions and Outlook

Using harpoon for anchorage on the surface of an asteroid has been studied which shows the bounce off phenomena for ordinary chondrite that constitutes the asteroid. The analysis shows that using harpoon for anchorage is not reliable. The study pointed to a new direction of the mechanical anchoring system, design a special harpoon lead to harpoon self-rotating after penetrating rock to anchor rock of Asteroids.

References

[1] Ziska, J., Yarkovsky and YORP Effects in Dynamics of Small Bodies of the Solar System. PhD thesis, 2018.
[2] Prado, J., Perret, A., Boisard, O., 2011. Deflecting Apophis with a flotilla of solar shields. Advances in Space Research 48 (11), 1911–1916.
[3] Howard, R., Gillett, R., 2007. A low cost rendezvous mission to 99942 Apophis. IEEE Aerospace Conference, 375-384, 3-10 March.
[4] Jonathan, S.T., Jonathan L.S., Jarret M.L., 2008. Cost-based launch opportunity selection applied to rendezvous with 99942 Apophis. 18th AAS/AIAA Space Flight Mechanics Meeting, Galveston, 28 January-1 February.
[5] Oliver, S., Massimiliano, V., Carlos A.C.C., 2011. Computing the Set of Epsilon-Efficient solutions in multiobjective space mission design. Journal of Aerospace Computing Information and Communication. 8 (3), 53-70.
[6] Nathues, A., Boehnhardt, H., Harris, A. W., Jentsch, C., Schaeff, S., Weischede, F., Wiegand, A., Schmitz, N., Goetz, W., Kachri, Z, 2010. ASTEX: An in situ exploration mission to two near-Earth asteroids. Advances in Space Research. 45 (1), 169-182.
[7] Duffard, R., Kumar, K., Pirrotta, S., Salatti, M., Kubinyi, M., Derz, U., Armytage, R.M.G., Arloth, S., Donati, L., Duricic, A., Flahaut, J., Hempel, S., Pollinger, A., Poulsen, S., 2011. A multiple-rendezvous, sample-return mission to two near-Earth asteroids. Advances in Space Research. 48 (1), 120-132.
[8] Ulamec, S., Espinasse, S., Feuerbacher, B., Hilchenbach, M., Moura, D., Rosenbauer, H., Scheuerle, H., Willnecker, R., 2006. Rosetta Lander- Philae: Implications of an alternative mission. ACTA Astronautica. 58 (8), 435-441.
[9] Ulamec, S., Biele, J., 2009. Surface elements and landing strategies for small bodies missions-Philae and beyond. Advances in Space Research. 44 (7), 847-858.
[10] Hilchenbach, M., Kuchemann., O., Rosenbauer, H., 2000. Impact on a comet: Rosetta Lander simulations. Planetary and Space Science. 48 (5), 361-369.
[11] Thiel, M., Stocker, J., Rohe, C., Komle, N.I., Kargl, G., Hillenmaier, O., Lell, P., 2003. The Rosetta Lander anchoring system. 10th European Space Mechanisms and Tribology Symposium, San Sebastian, 24-26 September.
[12] Biele, J., Ulamec, S., 2008. Capabilities of Philae, the Rosetta Lander. Space Science Reviews. 138 (1), 275-289.
[13] Kargl, G., Macher, W., Komle, N.I., Thiel, M., Rohe, C., Ball, A.J., 2001. Accelerometry measurements using the Rosetta Lander's anchoring harpoon: experimental set-up, data reduction and signal analysis. Planetary and Space Science. 49 (5), 425-435.
[14] Komle, N.I., Ball, A.J., Kargl, G., Keller, T., Macher, W., Thiel, M., Stocker, J., Rohe, C., 2001, Impact penetrometry on a comet nucleus - interpretation of laboratory data using penetration models. Planetary and Space Science, 49 (6), 575-598.

[15] Barnouin-Jha, O.S., Cheng, A.F., Mukai, T., Abe, S., Hirata, N., Nakamurad, R., Gaskell, R.W., Saito, J., Clark. B., 2008, Small-scale topography of 25143 Itokawa from the Hayabusa laser altimeter. ICARUS, 198 (1), 108-124.
[16] Nolan, M. C., Magri, C., Howell, E. S., et al, 2013. Shape model and surface properties of the OSIRIS-REx target Asteroid (101955) Bennu from radar and lightcurve observations. ICARUS, 226 (1), 629-640.
[17] Chesley, S. R., Farnocchia, D., Nolan, M. C., et al., 2014, Orbit and bulk density of the OSIRIS-REx target Asteroid (101955) Bennu. ICARUS, 235 (6), 5-22.
[18] Binzel, R. P., Rivkin, A. S., Thomas, C. A., et al. 2009. Spectral properties and composition of potentially hazardous Asteroid (99942) Apophis. ICARUS. 200 (2), 480-485.
[19] Delbo, M., Cellino, A., Tedesco, E.F., 2007. Albedo and size determination of potentially hazardous asteroids: (99942) Apophis. Icarus, 188 (1), pp. 266-269.
[20] Britt, D.T., Gonsolmagno, G.J., 2003. Stony meteorite porosities and densities: A review of the data through 2001. Meteoritics & Planetary. Science, 38 (8), 1161-1180.
[21] Britt, D.T., Yeomans, D., Housen, K., Consolmagno, G., 2002. Asteroid density, porosity, and structure. In: Bottke, W.F., Cellino, A., Paolicchi, P., Binzel R.P.(Eds), Asteroids III. University of Arizona Press, Tucson, pp. 485-500.
[22] Kimberley, J., Ramesh, K. T., 2011. The dynamic strength of an ordinary chondrite. Meteoritics & Planetary Science. 46 (11) , 1653-1669.
[23] Dai, C.D., Jin, X.G., Fu, S.Q., Shi, S.C., Wang, D.D., 1997, The equation-of-states of Jilin ordinary chondrite and Nandan iron meteorite. Science in China Series D-Earth Science. 40 (4), 403-410.